

# FIRST RESULTS FROM THE MAGIC EXPERIMENT

DENIS BASTIERI FOR THE MAGIC COLLABORATION\*

*Dipartimento di Fisica, Università di Padova  
& INFN Sezione di Padova,  
Via Marzolo 8 - 35131 Padova, Italy  
E-mail: bastieri@pd.infn.it*

The MAGIC Telescope after a full year of commissioning phase is now successfully taking data since October 2004. Many technical innovations contribute in lowering its energy threshold well below 100 GeV. Among them, the all-aluminium parabolic reflecting surface that, with its 236 m<sup>2</sup> makes it nowadays the biggest Cherenkov telescope and a smart trigger able to cope with the increased background rate. In this contribution, along with a brief overview of the scientific goals of MAGIC, details will be given on the construction and performance of the telescope, highlighting its first observational results and the potential for new physics.

## 1. Introduction

The MAGIC Telescope<sup>†</sup> was built at 2,200 m a.s.l. at the Observatorio del Roque de Los Muchachos (ORM) (28.8° N, 18.8° W), the site that, together with the Observatorio del Teide, makes up the so-called European Northern Observatory (ENO), a renown site for the high astronomical quality of the sky, due to the very low humidity and to minimal air turbulences.

In the construction of MAGIC, the **Major Atmospheric Gamma Imaging Cherenkov Telescope**, the collaboration aimed at lowering as much as possible the current energy threshold of ground detectors, in order to open for observation a new energy window of the electromagnetic spectrum between 30 and 250 GeV.

This energy window has as lower limit the upper energies observable by satellite-borne detectors. These experiments have to clash with the poor statistics of high-energy events and with the limited amount of weight available to calorimetric identification. This limit, of  $\sim 10$  GeV, was obtained

---

\*<http://magic.mppmu.mpg.de/collaboration/members/index.html>

†<http://magic.mppmu.mpg.de/>

on-board CGRO with EGRET and will be pushed somewhat up with the oncoming launches of AGILE[1] and GLAST[2].

Instead, ground-based experiments, and especially IACT (Imaging Atmospheric Cherenkov Telescopes) like MAGIC, are pulling the upper limit down. Ground experiments detect the shower development of primary particles in our atmosphere and not the primary particles themselves, as satellite-borne experiments do, thus, they have to rely on Montecarlo simulations in order to calibrate the algorithms for the energy reconstruction and particle identification. On the other hand, they are not limited by statistics, as their effective area is not the actual detector size, as for satellite ( $\sim 1 \div 10 \text{ m}^2$ ), but the cross section of the developing shower ( $10^{4+5} \text{ m}^2$ ).

It can be shown that the energy threshold of IACTs roughly scales down with the reflecting surface and correlated quantities (like reflectivity, conversion efficiency, ...). For this reason, modern IACT projects are all endowed of enormous surfaces: HESS<sup>†</sup>, CANGAROO III<sup>§</sup> and VERITAS<sup>¶</sup> feature  $10 \div 12 \text{ m}$   $\varnothing$  dishes. Besides them MAGIC, with a  $17 \text{ m}$   $\varnothing$  dish and a total reflecting surface of  $236 \text{ m}^2$ . Nevertheless, having huge surfaces is not enough to lower energy thresholds: as the *solar farm* case showed, one has also to cope with background, increasing consequently with the bigger area. In this contest, having a smart trigger that can reject a background fraction even at hardware level can be essential.

## 2. Scientific Subjects

Taking the burden of lowering the energy threshold has, as its counterpart, a new realm of observations[3]. The most prominent case are AGNs, that at EGRET energies are counted by dozens and populate different redshifts, while for older IACT detectors (like Whipple and HEGRA) did not show up beyond  $z \approx 0.03$ . These differences can arise from an internal cut-off of the AGN power-law spectrum between 20 and 250 GeV, or from interaction of the emitted gammas with the extragalactic background light. In this context MAGIC, that can detect in 50 hours at a  $5\sigma$ -level a source with a *Crab-like spectrum* and an integral flux of  $10^{-10} \gamma \text{ cm}^{-2} \text{ s}^{-1}$  as low as at 50 GeV, should observe plenty of AGNs and even discriminate between the two models (see Fig. 1 for an updated comparison of sensitivities of various experiments).

---

<sup>†</sup><http://www.mpi-hd.mpg.de/hfm/HESS/HESS.html>

<sup>§</sup><http://icrhp9.icrr.u-tokyo.ac.jp>

<sup>¶</sup><http://veritas.sao.arizona.edu>

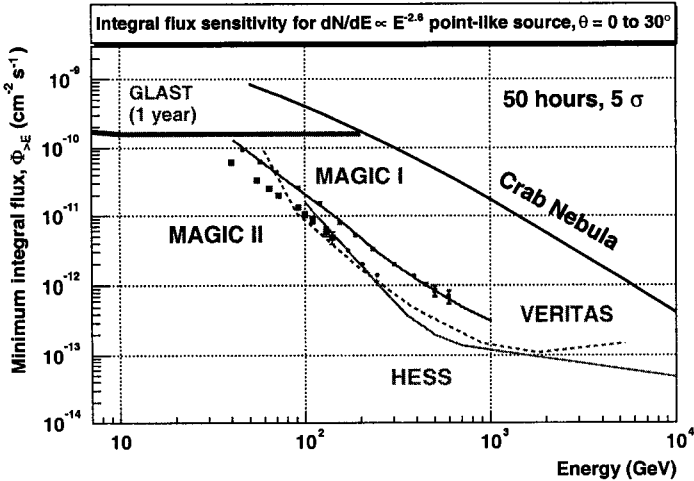


Figure 1. Predicted sensitivities for some operating and proposed detectors. Note the wide overlap between GLAST and present Cherenkov telescopes. As far as MAGIC is concerned, the solid, red line represents the predictions made by the full Montecarlo simulation, in good agreement with the sensitivity calculated from the first observations. Blue dots are the expected sensitivity for MAGIC II, a *clone* of the current MAGIC, that will be built at 85 m of distance from MAGIC. Start of operation for MAGIC II is envisaged for the beginning of 2007, just before the scheduled launch of GLAST.

Moreover, EGRET legacy consisted of plenty of unidentified sources, and observation stretching up the energy window could help knowing them. AGNs, alongside with other gamma emitters such as supernova remnants (SNRs) and microquasars can all fit in this class: a thorough study could bridge the energy gap between satellite and ground detectors and identify the main sources of cosmic rays up to an energy of  $10^6$  GeV.

Related to AGNs, or better to a catalogue of observed AGNs at different redshifts, is the measurement of many cosmological parameters. The *Hubble parameter* can have its more precise measurement in this way.

The interesting phenomenon of GRBs can be also a subject for MAGIC that, due mainly to its stiff and lightweight supporting cradle, can be re-pointed in less than 20 seconds. An early satellite follow-up, as the one provided by SWIFT, gives MAGIC the unique opportunity of an early follow-up ( $\lesssim 30$  s) at energies well below 100 GeV.

Finally, a low energy threshold, virtually inside satellite energy window, can help in calibrating the energy reconstruction methods that now deeply rely on Montecarlo techniques. Satellite experiments and their direct detection of cosmic rays can thus provide a sort of *test beam* for MAGIC[4].

### 3. The MAGIC Telescope

The MAGIC telescope is an international collaboration that among its main components enrolls Germany, Spain and Italy. MAGIC fits nicely in a frame of continuous monitoring in the hundred GeV region for both hemispheres, since the other three *second generation* collaborations are situated in Australia (CANGAROO), southern US (VERITAS) and Namibia (HESS). It features a reflecting surface of parabolic shape  $F/1$  and  $236\text{m}^2$  of size, made up with 964 aluminium mirrors, of  $80 \div 90\%$  reflectivity. The collected light is focused in a camera equipped with 576 6-dynode compact photomultipliers, featuring  $\sim 20\%$  of quantum efficiency in the  $300 \div 500\text{ nm}$  band[5].

A two-level trigger system[6] takes care of removing most of the background light, and start the conversion to digital data. Pixel signals are stretched and converted with a high and a low gain to enlarge the dynamic range. The final digitisation is done using 300 MHz 8-bit flash ADCs. The maximum readout rate is around 1kHz, for a total of 80GB of data collected on the longest nights ( $\sim 11$  hours). The typical readout rate of collected data is instead much lower,  $250 \div 350\text{ Hz}$ , taking into account also a 50 Hz rate of calibration events.

The telescope features also a very lightweight mount, mainly made with a *filigree* structure of carbon fibre tubes jointed together onto aluminium ball-nodes. The resulting structure is very stiff, reacting to 10 m/s wind gushes with a  $\sim 3\text{ cm}$  maximal displacement of the camera. On the other hand, being so lightweight, MAGIC can promptly react to *ToO* (Target of Opportunity) such as GRB alerts, as was the case of GRB 050723, simultaneously observed with SWIFT during the flaring activity.

### 4. First observations of sources and performance on data

The first sources observed were the Crab Nebula and MKN 421. Both of these sources are a sort of *standard* sources: the Crab is a *plerion*, a SNR hosting a pulsar in its core, and has a steady flux that can be used to calibrate detectors. MKN 421 is a very close AGN ( $z = 0.03$ ) and, while not being steady, stays from time to time in a high state with fluxes few times bigger than the Crab one. They were observed even in the commissioning phase in Winter 2003/2004 (the Crab Nebula) and during Spring 2004 (MKN 421) and both revealed signals well above the  $5\sigma$  level.

The Crab and MKN 421 were also observed later on, during the first semester of data acquisition. In addition, another AGN, 1ES1959+650, farther than MKN 421, was detected even if it was quiescent.

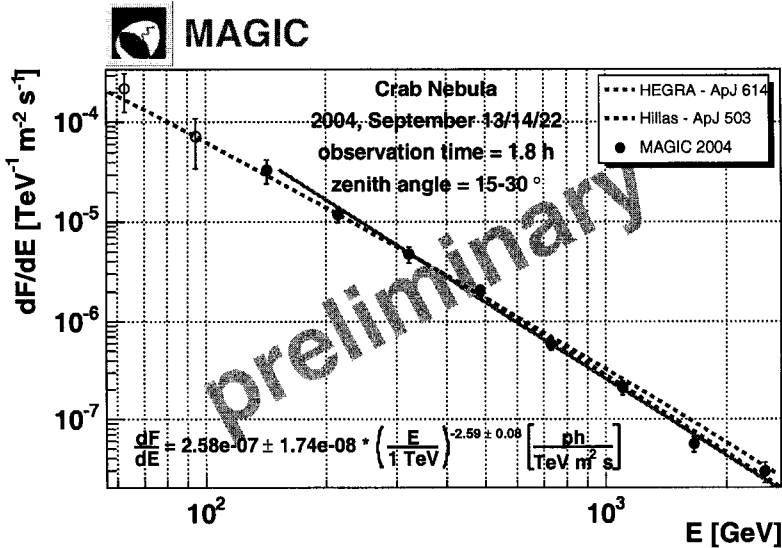


Figure 2. Preliminary Crab spectrum obtained after analysing 2 hours of data taken September between 15° and 30° of zenith angle. The grey line corresponds to the fitted formula.

#### 4.1. The Crab Nebula

The *Crab Nebula* is nowadays the standard candle for VHE (Very High Energy) gamma astronomy, having a steady flux since many years. In this energy range the emission is mainly due to the Inverse Compton Scattering of the synchrotron radiation. The observation at low energies should allow the study of the Compton peak, of interest for many theoretical models.

Given the importance of the Crab Nebula, mainly for calibration purpose and for the aforementioned Compton peak, MAGIC enlisted the Crab as its first scheduled object, even during the first semester of the physics campaign.

Collected and analysed data showed the presence of a signal even at low energies (< 100 GeV) (see Fig. 2). The entity of systematic errors is still under evaluation, even if we do not expect a substantial modification of the proposed spectrum especially at high energies.

#### 4.2. Markarian 421

While on commissioning phase, on April 22<sup>nd</sup>, 2004, MKN 421 was in a high state. Data collected during that night, with MAGIC pointing at

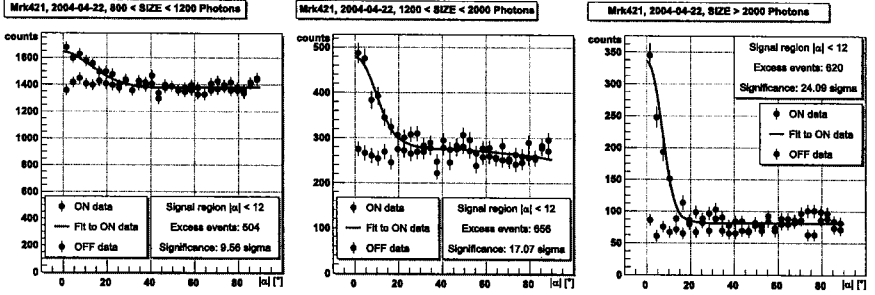


Figure 3. Data from 155-minutes of acquisition taken on April 22<sup>nd</sup>, 2004 with MAGIC pointing at MKN 421. The histogram of  $\alpha$  for on- and off-source observations, are relative to different bin in  $size$ : 800–1200 (left), 1200–2000 (middle) and more than 2000 photons (right).

the source, are shown in Fig. 3. MAGIC, as all IACTs, records for each event the directions of the Cherenkov photons emitted during the shower development. The image is then analysed using a well-established technique that exploits the so-called *Hillas parameters*[7].

Two Hillas parameters have a particular importance in the figure:  $\alpha$  and  $size$ .  $\alpha$  is related to the actual direction of the primary particle that initiated the shower, thus an excess in  $\alpha$  must be seen in the direction of a source.  $Size$  is the number of photons making up the image and is related to the energy of the primary particles (the more energetic is the particle, more photons appear in the image).

The three figures show that the MKN 421 flare was well detected by MAGIC at different energies, and the excess seen in the first figure with  $size$  ranging from 800 to 1200 photons is consistent with an energy well below 100 GeV.

Observation made afterward, during the physics campaigns, featured a joint observation with HESS. On December 2004, the X-ray satellite RXTE reported the high state of MKN 421. The AGN was repeatedly observed by many ground detectors in many different wavelengths. Among them MAGIC and HESS that were able, on December 18<sup>th</sup>, 2004, to observe simultaneously the source, allowing:

- a mutual cross calibration of the two experiments, that could help in understanding and reduce systematic errors;
- a simultaneous observation in two different energy ranges, as the source was visible to the two experiments at different zenith angles.

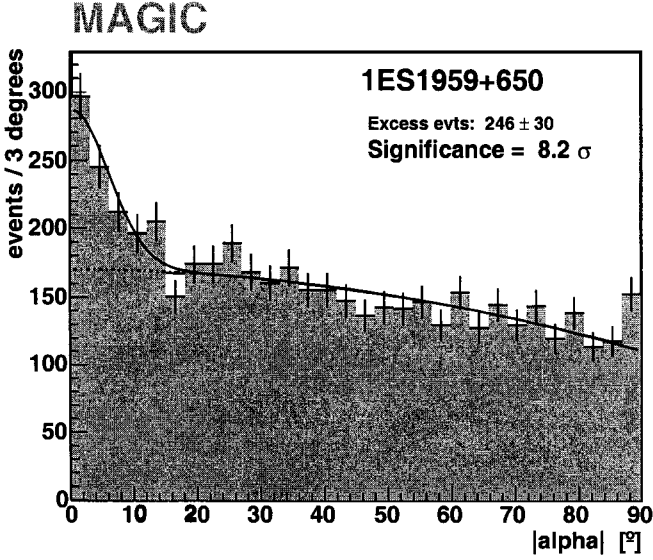


Figure 4.  $\alpha$  plot of 1ES1959+650 after cuts on image parameters. The graph shows the second-order curve used for estimating the background at low  $\alpha$  (up to  $9^\circ$ ).

#### 4.3. 1ES1959+650

The AGN 1ES1959+650 is an X-ray peaking *BL Lacertae* object selected from the Einstein Medium Sensitivity Survey. It is hosted by an elliptical galaxy at a redshift of  $z = 0.047$ .

MAGIC has observed VHE gamma-ray emission from 1ES1959+650 during six hours in September and October 2004. The observations were carried out alternated with the *Crab Nebula*, whose data were used as reference source for optimising gamma/hadron separation and for flux comparison. The data analysis shows VHE gamma-ray emission of 1ES1959+650 with  $\sim 8\sigma$  significance, at a time when the AGN was reported to be quiescent in both optical and X-ray wavelengths (see Fig. 4).

An integral flux above  $\sim 180$  GeV of about 20% of the Crab was obtained. The light curve, sampled over 7 days, shows no significant variations. The differential energy spectrum between 180 GeV and 2 TeV can be fitted with a power law of index  $-2.72 \pm 0.14$ . The spectrum is consistent with the slightly steeper spectrum seen by HEGRA at higher energies, also during periods of low X-ray activity.

## 5. Conclusions

The MAGIC telescope has started its regular operation. Designed to be a pioneering telescope for low-energy gamma astronomy, it is now giving its first results. Several sources were detected, among them the *Crab Nebula* that presumably can be studied even close to the Compton peak and the *medium*-far AGN 1ES1959+650, that even if quiescent and at a flux level of  $\sim \frac{1}{10}$  Crab was well detected in 6 hours.

New analysis tools, including timing info, are under study, to work at lower energies and further enhance the instrument sensitivity.

Given the success of the detector, the MAGIC Collaboration started the construction of a second detector (MAGIC II) to be built at a distance of 85 m from the current MAGIC telescope. Start of operation for MAGIC II is envisaged for the beginning of 2007, just before the scheduled launch of GLAST.

## Acknowledgments

The construction of the MAGIC Telescope was made possible by the financial contributions of the Italian INFN, the German BMBF and the Spanish CICYT, to whom goes our grateful acknowledgement. We would also like to thank the IAC for the excellent working conditions provided at El Roque de los Muchachos.

## References

1. M. Tavani et al. (2001), Procs. Symp. *Gamma 2001*, S. Ritz, N. Gehrels, C.R. Shrader eds., AIP Conf. Proc. 587, 729.
2. P. Michelson et al. (1999), Response to AO 99-OSS-03, GLAST Large Area Telescope, Flight Investigation: An Astro-Particle Physics Partnership Exploring the High-Energy Universe Volume 1: Scientific and Technical Plan.
3. A. Saggion and D. Bastieri, "*The Observational Energy Gap between 10 and 300 GeV*", *Mem. Soc. Astro. It.* 73/4 (2002), pp. 812–821.
4. D. Bastieri et al, *Astropart. Phys.* 23/6 (2005), pp. 572–576, arXiv:astro-ph/0504301.
5. A. Ostankov et al, *Nucl. Inst. & Meth.* A 471 (2001), pp. 188–191.
6. D. Bastieri et al, *Nucl. Inst. & Meth.* A 461 (2001), pp. 521–523.
7. A.M. Hillas (1985), Procs. 19<sup>th</sup> ICRC, La Jolla, USA 1985, vol. 3, p. 445–448.

# H.E.S.S.

P. VINCENT FOR THE H.E.S.S. COLLABORATION

*Laboratoire de Physique Nucléaire et de Hautes Energies,  
IN2P3/CNRS, Universités Paris VI & VII,  
4 Place Jussieu, F-75252 Paris Cedex 05, France*

The first phase of the H.E.S.S. experiment is now fully operational since the end of 2003 but observation has started in mid 2002. After a systematic study of known TeV sources in the southern hemisphere, the H.E.S.S. collaboration has undertaken a scan of the inner region of the galactic plane. It also accomplished observations of many other galactic and extragalactic objects. We report here on the observation periods between 2003 and 2004.

## 1. Introduction

The H.E.S.S. experiment[1] is an array of four Imaging Atmospheric Cherenkov Telescope installed in the Khomas district in Namibia. Each telescope[2] has a large Davis-Cotton mirror of 108 m<sup>2</sup> area fixed on a alt-azimuth mount. The focal plane is equipped with a camera[3] of 960 photo-multipliers for a total field of view (FoV) of 5°. This large FoV is specially propitious to the observation of extended sources like supernovae remnant (SNR) and also favourable to observations in scan mode or to search for new sources of high energy gamma rays. The angular resolution of individual shower reconstruction is about 0.1° and the precision in the determination of the source position is better than 1'. With a threshold of about 100 GeV and a sensitivity at the level of a percent of a Crab-like source; this experiment has reached its objectives concerning performance. On the site of operation, an online analysis based on a preliminary online calibration chain gives an indication on the significance of the tracked objects after one hour. However, all the analyses presented here or published in reviews are based on two independent offline calibration chains developed in parallel to check our understanding of the apparatus and also use three different methods of analysis. The first one is based on Hillas parameterisation of shower images followed by a geometrical reconstruction of the shower axis[4]. The two other methods[5,6] used full two or three

dimensional models to predict the Cherenkov light emitted by gamma-ray initiated air showers and perform a fit to each experimental image to find the best parameters of the initial photon (see also [7] for comparison of these three methods). The efficiency of the source reconstruction is better than 50% in the inner  $3^\circ$  region of the FoV and some analyses based on the analytical model have demonstrated the possibility to reconstruct sources located at the edge of the total FoV. Between 2003 and 2004, the H.E.S.S. collaboration have tracked more than one hundred targets for a total of about 1,000 hours of observation time per year. A scan of a small inner region of our galaxy has been carried out[8] in the range of  $\pm 30^\circ$  of galactic longitude and  $\pm 3^\circ$  in latitude. The result of this scan is shown in figure 1. A total of eleven sources have a significance higher than  $6\sigma$  (white labels), and also seven hot spots at more than  $4\sigma$  are present in this scan (in yellow). Galactic sources, outside this region, were also observed

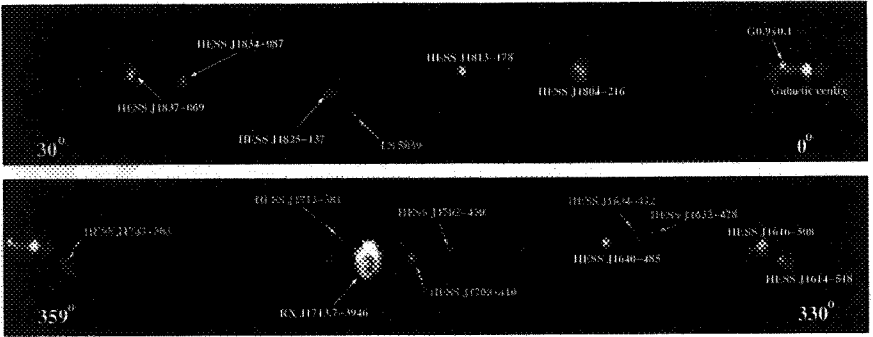


Figure 1. H.E.S.S. scan of the central region of the Milky Way. The top figure shows the scan from  $-30^\circ$  to  $+2^\circ$  and bottom scan from  $-2^\circ$  to  $+30^\circ$ .

and detected; whereas some source remains undetectable like, for instance, the SNR **SN1006** and the pulsar wind nebula (PWN) **PSR B1706-44**. They has been observed and upper limits have been published[9,10]. Extragalactic observations has been carried out for several blazars as well as non-blazar targets bringing new results. These observations have been used to constrain the level of extragalactic background light[11]. In this paper we will not cover all these topics; the reader is invited to refer to published papers in references and also to the proceeding of the ICRC conference[12] for the latest H.E.S.S. result.

## 2. Galactic sources

The H.E.S.S. observations have allowed for the first time in this domain the source morphology. This is particularly important to understand the location of the gamma production and to identify the surrounding environment of these sources. To carried out such analysis one must achieve a high position resolution as well as collecting a sufficient data sample. With the accuracy of the position reconstruction and the sensitivity of the H.E.S.S. apparatus these two conditions are fulfilled. Figure 2 show two spectac-

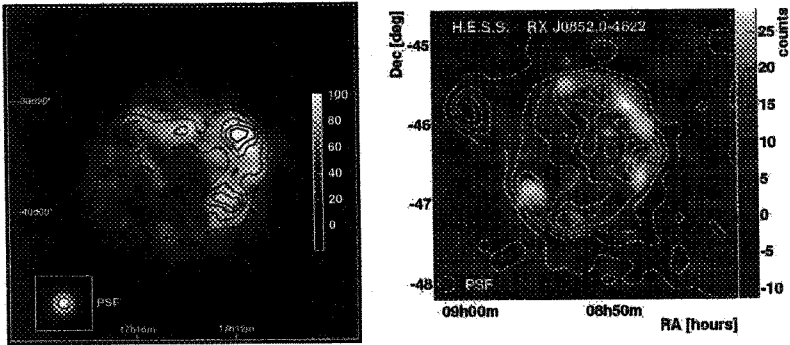


Figure 2. H.E.S.S. excess map of RX J1713-3946 (left) and RX J0852.0-4622 (right). The superimposed white lines indicate the contour in X-rays from ASCA (RX J1713) and ROSAT (Vela). The image is smoothed with a Gaussian of 2 arcmin standard deviation, the linear colour scale is in units of excess counts.

ular demonstrations of this performance. On left, a  $2^\circ \times 2^\circ$  field of view centred on the SNR **RXJ 1713-3946**[13] is shown. Initially discovered by the satellite ROSAT in an all-sky-survey X-rays at about 1 kpc, this object has been later claimed as source of TeV gamma rays by the CANGAROO collaboration[14]. The distributed gamma emission is similar to a shell morphological structure with no clear evidence of any emission from the central region. It demonstrate that shocks generated by supernovae can accelerate charged particles up to multi-TeV energies producing secondary high energy gammas by interaction with the interstellar medium in case of protons or inverse compton process for electrons. The overall shell structure coincides with that seen in X-ray contours (from ASCA) which indicates that the two type of emission have a similar origin. The overall gamma-ray flux corresponds to about 66% of the flux of the Crab Nebula as measured with H.E.S.S. This distribution shows a significant asymmetry between a brightest part (with an excess of  $20\sigma$ ) in the West and northwestern region of the map and the southeastern region. It is believed that in the

highest emitting region, interaction with dense molecular clouds enhance the gamma ray production. **RX J0852.0-4622** (Vela Junior), previously announced by the CANGAROO collaboration at TeV energies[15], is another interesting example of shell structure emitting object. The right of figure 2 shows the excess map reconstructed by the H.E.S.S. detector[16]. From the galactic scan a total of eighteen sources, sixteen of which are new, have been discovered. Three of them were clearly identified in this scan and associated with known SNR in other wavelength. **HESS J1640-465** is a marginally extended source with respect to the H.E.S.S. point spread function. Its flux is close to 9% of the Crab above 200 GeV, with a spectral index of  $2.42 \pm 0.15$ . Its position is closely correlated with the SNR G338.3-0.0. It is also compatible with 95% confidence contour of the EGRET source 3EG J1639-4702, and its spectrum extrapolated down to 1 GeV is compatible. Two other SNR candidates are **HESS J1804-216**, a bright source at 20% of the Crab and **HESS J1834-087**, a faint gamma emitter at 5% of the Crab. They are both extended with a size of 22 and 12 arc minutes respectively with similar spectral index. The first can be associated with the South-Western part of the shell of G008.7-00.1, but it also coincides with the pulsar PSR J1803-2137. The second positionally coincides with the shell-type SNR G023.3-00.3.

Stellar object where gamma rays are generated in pulsar wind nebulae, similar to the Crab Nebula, are another class of TeV emitters. Among them, the source termed **HESS J1825-137**, initially announced as an unidentified TeV source, has been recently associated to the close but not clearly coincident pulsar PSR B1823-13[17]. This pulsar, with an estimated distance of about 4 kpc, reveals an asymmetric spatial distribution of TeV gamma rays, peaking at the pulsar position and decaying toward the South. This behaviour is remarkably similar to the situation in X-rays, where the pulsar is surrounded by a nebula with a pronounced tail toward the South, except that the scales are different. Relativistic electrons and positrons are presumed to be ejected symmetrically from the pulsar, but the north jet was crushed by a reverse shock rebounding when the supernova shock wave had piled up enough interstellar material. When expanding into an inhomogeneous medium, the reverse shock from the (lower-density) South side may not yet have reached the PWN[18]. The SNR **MSH 15-52** was first discovered in radio observations[19]. It reveals a roughly circular supernova shell with a bright emission in the North-West rim and a fainter one in the South-East. At the centre of the shell, a 150 ms X-ray pulsar (PSR B1509-58) remains from the supernova explosion. The pulsar is surrounded

by a diffuse nebula of unpulsed X-ray emission, similar to that observed in the Crab nebula. The Chandra X-ray image[20] shows a jet-like structure emerging from the pulsar with a collimated outflow arc-like structures in the North of the pulsar. In 2004, about 22 hours of data were accumulated on

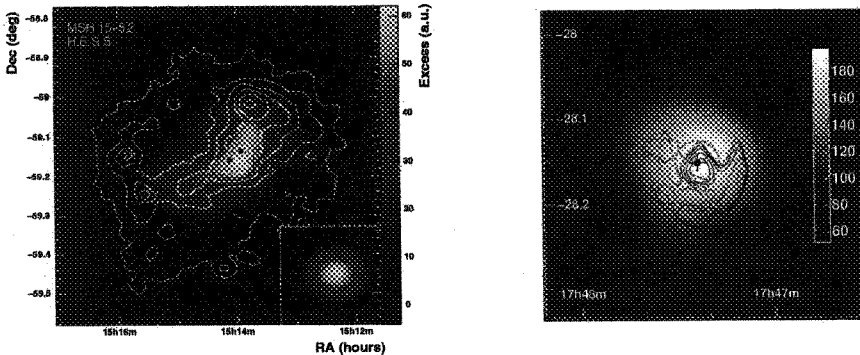


Figure 3. H.E.S.S. excess map of MSH 15-52 (left) and G00.9+00.1 (right). The superimposed white lines indicate the contours in X-rays from ROSAT. The image is smoothed with a Gaussian of 2 arcmin standard deviation, the linear colour scale is in units of excess counts.

MSH 15-52, showing a clear TeV gamma-ray signal[21] with a significance of 25 sigma and a flux of roughly 15% of that observed for the Crab Nebula. The TeV gamma rays show a clearly resolved structure (Fig. 3, left), with an elongated and slightly curved emission region, similar to the morphology of the X-ray jet. In the North-West direction, the source has a characteristic width of 6' (assuming a Gaussian source profile), and in the orthogonal direction a width of about 2'. The centre of gravity of the gamma-ray emission is displaced from the pulsar. In 2003, first observations of the Galactic Centre region with two H.E.S.S. telescopes already showed a faint signal at the location of **G00.9+00.1**[22]. In 60 h of follow-up observations between March and September 2004, with all four H.E.S.S. telescopes, a highly significant signal is detected (13 sigma), consistent with the position of the core of the SNR (Fig. 3, right). Within the angular resolution of H.E.S.S., the source is point-like, with an emission region smaller than 1.3' (rms). The location of the source and the size limit strongly suggest the PWN as the source of the VHE gamma-ray signal, rather than the supernova shock wave.

In the vicinity of the binary system PSR B1259-63/SS 2883, discovered by the H.E.S.S. collaboration[23], the experiment, equipped with camera of 5° of FoV has, in 2004, detected simultaneously a second object which

is unidentified in any other wavelength. This new object, called **HESS J1303-631**, exhibits an hard spectrum of  $2.4 \pm 0.2$  and a strong signal with a flux of 17% of the Crab. It has been observed in 2004 with a significance of  $13 \sigma$  level at 0.7 degrees to the North of the binary system[24]. Several pulsars are known with positions close to HESS J1303-631. However, from the energetics point of view, most of them are ruled out apart PSR J1301-6305 which remain a interesting candidate. Up to now, no other plausible candidates such as dense gas clouds illuminated by cosmic rays or dark matter annihilation clumps match this signal. More sensitive follow-up measurements in other wavelength regimes might help to pin down the physics of this new source. Another unidentified source from the galactic scan is **HESS J1614-518**, with a reconstructed mean size of  $12 \pm 1$  arc minutes with elliptical morphology. It was identified at galactic longitude  $331.52 \pm 0.03$  and latitude  $-0.58 \pm 0.02$ , close to the pulsar PSR J1617-5055. It is the brightest source of the scan with a flux of about 25% of the Crab Nebula flux. Its spectrum fit a power law with photon index  $2.46 \pm 0.20$ . The observation of a region of 10 arc minutes around the location of this source by the Chandra X-ray satellite does not show any evidence of X-ray emission in the direction of this source. The galactic centre has been

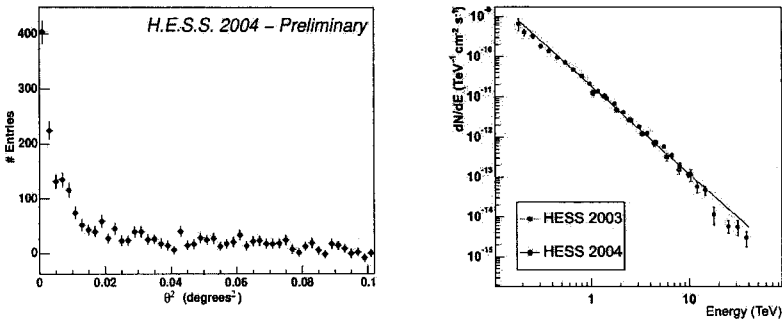


Figure 4. Excess of gamma-ray candidates in the H.E.S.S. data (left) in the direction of the Galactic centre and reconstructed energy spectrum (right).

observed continuously in 2003 and 2004[25]. The reconstructed spectrum exhibit the same spectral index and the flux seems stable over all time-scales. In the distribution of the gamma-ray excess we can see two components, a narrow profile close to the position of the source super-imposed on an extended tail. Various attempts to fit this distribution with predicted profile from dark matter annihilation failed, and more classic gamma-ray production processes must be envisaged to explain the observed signal.

### 3. Extra-galactic sources

From the H.E.S.S. site, **Mkn 421** ( $z = 0.031$ ) is observed[26] at large zenith angle. With a reconstructed flux of about 3 Crab above 2 TeV, the data corresponding to 15 hours of observation allows a clear detection of  $100\sigma$ . The light-curve in April and May exhibit significant intra-night variability. These observations were taken with a zenith angle between  $60^\circ$  and  $67^\circ$  which results a large collection area ( $2 \text{ km}^2$ ) at 10 TeV specially appropriate to study the effect of gamma ray absorption by extra-galactic background light on the end-point energy spectrum. The reconstruction spectral curvature can be described by a power law ( $2.1 \pm 0.1 \pm 0.3$ ) with an exponential cut-off at  $3.1(+0.5-0.4) \pm 0.9$  TeV or super-exponential cut-off at ( $6.25 \pm 0.4 \pm 0.9$ ) TeV. The blazar **PKS 2005-489** ( $z = 0.071$ ) has been detected[27] at a signal level of  $6.7 \sigma$  in a sample of 24.2 hours live-time, which corresponds to 2.5% Crab flux. It is the first blazar independently discovered by H.E.S.S. at TeV energies and the second in the southern hemisphere. No evidence for variability at the scale of a year was seen. The energy spectrum ( $\Gamma = 4.0 \pm 0.4$ ) corresponds to a particularly soft emission for a BL Lac. The detection of **PKS 2155-304**[28] ( $z = 0.117$ ) was confirmed at more than  $90 \sigma$  in 2004, with a soft power law shape. Two multiwavelength (MWL) campaigns took place in 2003 and 2004. In 2004 the variability was sufficient to suggest a correlation between X-rays and  $\gamma$ -rays activity and also to probe intra-night variability. MWL observations also indicate that **PKS 2155-304** was in a low or quiescent state during some observations periods. Finally, the nearby radio Galaxy **M87** located at a red shift of 0.004 was detected at a significance level of  $4.6\sigma$ [29]. The estimated flux of this source is between 0.5 and 1% of the Crab flux. With a jet oriented  $20^\circ$ - $40^\circ$  away from the observer's line of sight, this is a confirmation of the first non blazar extra-galactic source identified at TeV energies from the HEGRA collaboration[30], but more data are needed to state on a possible variability of the emission. Finally, the Seyfert galaxy **NGC 253** was observed during 28 hours and an upper limit has been recently published[31] well below the previous detection claimed by CANGAROO. Also, 19 BL Lacs and other AGNs at a red-shift between 0.002 and 0.3 has been observed and upper limits, between 1 and 3% of Crab flux, have been published[32] based on the analysis of 1 to 5 hours of observation time.

#### 4. Conclusions

The H.E.S.S. experiment is the most sensitive ground based detector of high energy  $\gamma$ -rays above 100 GeV. Studies of the Southern sky at TeV energies have been underway for a few years now and reveal for the first time the morphology of TeV galactic sources like shell-type SNR, pulsar wind nebulae or the galactic centre. The scan of the galactic plane brought an abundance of new sources of which some without clearly identified counterparts. On the extra-galactic side, a non-blazar TeV source has been confirmed and multi-wavelength campaign on AGN are undertaken with H.E.S.S. All these results stimulate the research and understanding of VHE  $\gamma$ -rays sources.

#### Acknowledgements

We would like to thank all the institutions that support the H.E.S.S. project and the PHD students, the PostDoc and the technical staff who contribute in a major part to the success of this experiment.

#### References

1. W. Hofmann et al., 2003, Proc. 28th ICRC, Tsukuba, p. 2811.
2. K. Bernlöhr et al., *Astropart. Phys.* 20 (2003) 111.
3. P. Vincent, et al., 2003, Proc. 28th ICRC, Tsukuba, p. 2887.
4. W. Benbow, 2004, 3rd Gamma-ray Inter. Symp. (Heidelberg), 611.
5. M. de Naurois et al., 2003, Proc. 28th ICRC, Tsukuba, Vol. 5, p. 2907.
6. M. Lemoine-Goumard et al., 2004, 3rd Gamma-ray Inter. Symp. (Heidelberg), 697.
7. M. de Naurois, Proc. of Cherenkov 2005, Palaiseau, (to be published).
8. F. Aharonian, et al. (H.E.S.S. coll.), *Science* 307 (2005) 1938.
9. F. Aharonian, et al. (H.E.S.S. coll.), *Astron. Astrophys.* 437 (2005) 135.
10. F. Aharonian, et al. (H.E.S.S. coll.), *Astron. Astrophys.* 432 (2005) 9.
11. F. Aharonian, et al. (H.E.S.S. coll.), 2005, astro-ph/0508073.
12. W. Hofmann et al., 2005, Proc. 29th ICRC, Pune, India, (to be published).
13. F. Aharonian, et al. (H.E.S.S. coll.), *Nature* 432 (2004) 75.
14. Enomoto, R., et al., *Nature*, 416, 823, 2002.
15. Watanabe S., et al. 2003, Proc. 28th ICRC, Tsukuba, p. 2397.
16. F. Aharonian, et al. (H.E.S.S. coll.), *Astron. Astrophys.* 437 (2005) 7.
17. F. Aharonian, et al. (H.E.S.S. coll.), *Astron. Astrophys.*, (to be published).
18. J. M. Blondin et al., *Astrophys. Journal*, Vol 563, Issue 2, p. 806.
19. J. L. Caswell et al., *Royal Astron. Soc.*, vol. 195, Apr. 1981, p. 89.
20. B. M. Gaensler et al., *Astrophys. Journal*, Vol 569, Issue 2, p. 878.
21. F. Aharonian, et al. (H.E.S.S. coll.), *Astron. Astrophys.* 435 (2005) 17.
22. F. Aharonian, et al. (H.E.S.S. coll.), *Astron. Astrophys.* 432 (2005) 25.
23. F. Aharonian, et al. (H.E.S.S. coll.), *Astron. Astrophys.* 442 (2005) 4.

24. F. Aharonian, et al. (H.E.S.S. coll.), *Astron. Astrophys.* 439 (2005) 1013.
25. F. Aharonian, et al. (H.E.S.S. coll.), *Astron. Astrophys.* 425 (2004) 13.
26. F. Aharonian, et al. (H.E.S.S. coll.), *Astron. Astrophys.* 437 (2005) 95.
27. F. Aharonian, et al. (H.E.S.S. coll.), *Astron. Astrophys.* 436 (2005) 17.
28. F. Aharonian, et al. (H.E.S.S. coll.), *Astron. Astrophys.* 430 (2005) 865.
29. M. Beilicke et al., 2005, Proc. 29th ICRC, Pune, India, (to be published).
30. F. Aharonian, et al. (HEGRA coll.), *Astron. Astrophys.* 403 (2003) 1.
31. F. Aharonian, et al. (H.E.S.S. coll.), *Astron. Astrophys.* 442 (2005) 177.
32. F. Aharonian, et al. (H.E.S.S. coll.), *Astron. Astrophys.* 441 (2005) 465.